

# Electron Transfer in Solid State Materials I

*S. H. Ehrlich  
12 Courtenay Circle  
Pittsford, New York 14534, USA*

## Abstract

This paper has related silver halide (AgBr, AgCl,  $\beta$ AgI) band gap energies to the common reference vacuum level and also the standard potential for redox couples referenced to the normal hydrogen electrode. This relationship suggests the thermodynamic limitations for photoreactions that can be carried out with charge carriers in the photographic silver halide microcrystals and other semiconductor materials of known band gap values. The author has not calculated mean field interactions such as the various aspects of intercalation or interaction energies that a given ion would feel if adjacent sites were full. Iridium III, rhodium III, and iodide energies from literature values are reasonably placed within the band gap of AgBr in order to support the understanding of photophysical electron transfer within heterogeneous, two-phased photosensitive systems and other imaging systems.

## Introduction

In general, an electron transfer may occur between a semiconductor electrode and a donor or acceptor in solution. The more specific case at hand is the photoexcitation of a silver halide microcrystallite and the transfer of the electron from the solid phase, the electrode, which serves as an electron sink or source. Alternatively, the redox reaction could take place in or at the interface of the nanoheterogeneous system or quantum cluster. The solid state properties of these imbedded aggregates depend strongly on the cluster size and the environment immediately surrounding these clusters; i.e., intercalation and mean field expressions for short-range crystal lattice. The charge at the interfaces controls the thermodynamics and kinetics of the heterogeneous redox reactions. The electrical field due to these charges at the interface is the major difference with respect to homogenous analogues. The photoexcitation with ensembles of relatively small numbers often fail to statistically represent all the host aggregates that may remain isolated with respect to the reaction time scale; thus, a variation of activation energies. Another interesting feature of these heterogeneous systems is the localization or position restriction of the epitaxial clusters in or upon the surface of the host crystal; e.g., faces, corners or edges of the crystals.

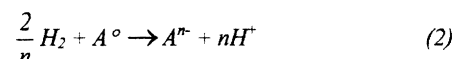
This paper describes an attempt to assemble a large quantity of data and present some possible correlation with respect to several potential photographic or imaging systems.

## Discussion and Results

The discussion centers around the Fermi level of a redox electrolyte expressed in terms of electrochemical potentials under standard conditions and the relation

$$E_f^{\circ}(\text{redox}) = \mu_{A^{n-}}^{\circ} - \mu_A^{\circ} - nF\phi_{\text{solution}} \quad (\phi, \text{Galvani potential}) \quad (1)$$

to the standard redox potential of the  $A^{\circ}/A^{n-1}$  redox couple. The normal hydrogen electrode (NHE) in electrochemistry is used as a reference. The Gibbs free energy  $\Delta G_{\text{NHE}}^{\circ}$  of the solution reaction describes the redox potential  $E_{\text{NHE}}^{\circ} (A^{\circ}/A^{n-})$  or



under standard conditions, where

$$\Delta G_{\text{NHE}}^{\circ} = -nFE_{\text{NHE}}^{\circ} \quad (3)$$

The vacuum or absolute potential scale is sometimes utilized instead of expressing redox potentials with respect to NHE. In the former case, the equilibrium



where

$$\Delta G_{\text{vac}}^{\circ} = \mu_{A^{n-}}^{\circ} - \mu_A^{\circ} = -nFE_{\text{vac}}^{\circ} \quad (5)$$

assuming the chemical potential of the electron at rest in vacuum, at infinite distance from the electrodes is zero. Comparisons of Eqs. 1 and 5 yields

$$E_f^{\circ}(\text{redox}) = -nFE_{\text{vac}}^{\circ} - nF\phi_{\text{solution}} \quad (6)$$

which shows the Fermi level of the electron in solution is not identical with the redox potential expressed on the vacuum scale. In the field of photoelectrochemistry, it is frequently asserted that these quantities are identical.<sup>1</sup> Bockris and Khan<sup>2</sup> pointed out that only in the unlikely case where the inner solution potential, Galvani potential, is zero does the condition  $E_f^{\circ}(\text{redox}) = -nFE_{\text{vac}}^{\circ}$  hold, as shown in Eq. 6.

Relating  $E_{\text{vac}}^{\circ}$  to  $E_{\text{NHE}}^{\circ}$  is accomplished by adding Eq. 7 to

$$ne_{-vac} + (nH^+)_{water} = \left(\frac{2}{n} H_2\right)_{water} \quad (7)$$

Eq. 2 and obtaining Eq. 4 for which the standard free energy is known to be  $-n(4.5 \pm 0.3)\text{eV}$ .<sup>3</sup> In order to convert a redox potential measured against the normal hydrogen electrode (NHE) to that expressed on the vacuum scale, the following relation is given, Eq. 8. A recent series of papers discussing conversion of

$$E_{vac}^\circ = E_{NHE}^\circ + 4.5 \quad (8)$$

relative to absolute potentials are listed.<sup>4-6</sup>

The increasing order of positive potentials beginning with 0.0 and ending with +5.5 V describes the ease of reduction; whereas the reduction reactions having reduction potentials more negative than that of the standard hydrogen electrode, beginning with 0.0 and ending with -1.5 V, describes the increasing difficulty of reduction. The standard electrode potential of an electrode reaction  $E^\circ(M^{n+}/M^\circ)$  is the standard potential of a reaction in a cell whose left-hand electrode is a hydrogen electrode (IUPAC) convention. The convention is noted by  $E^\circ(S/S^{2-}) = -0.47627$  V or  $E^\circ(S_n^{2+}/Sn) = -0.1364$  V with the temperature at 298.15 K under standard conditions of concentration; e.g.,  $C^\circ$  is  $1 \text{ mol L}^{-1}$ ,  $C^\circ \rightarrow 0$  and  $a_A^\circ = 1$ .

The energy levels for the conduction bands of AgBr, AgCl, and  $\beta\text{AgI}$  are 4.57, 4.59 (3% iodide), 4.51, and 3.90 eV, whereas the valence level measurements for AgBr,  $\text{AgBr}_{97}\text{I}_3$ ,  $\text{AgBr}_{74}\text{I}_{26}$ , AgCl, AgI indicate 7.14, 7.04 (3% iodide), 6.90 (26% iodide), 7.55, and 6.60 eV, respectively (Figures 1 and 2)<sup>7,8a</sup> (dashed lines). Normal hydrogen electrode potentials have been taken from the literature.<sup>8b</sup> However, solid state analysis and photographic sensitization experiments (solid lines) have yielded 3.30, 3.30, and 3.90 eV for conduction band determinations. The valence energy levels for the earliest measurements were taken to be 5.87, 6.50, and 6.75 eV, respectively. The band gap for several semiconductors have also been taken from the literature.<sup>8c,d</sup> But using the values published by Tejeda et al.<sup>9</sup> (AgCl 3.1 eV, AgI 3.7 eV) reverses the relative positions of the conduction bands of the first mentioned data of Bauer and Spicer.<sup>7</sup>

The solid state properties of imbedded aggregates depend strongly on the cluster size and the environment immediately surrounding these clusters and may be described by terms within an overlap wavefunction model of the holes and electrons between different atoms or ions,<sup>10-17</sup>

$$Eg(R) = Eg(R = 00) + \frac{h^2}{2} \frac{H^2}{R^2} \left[ \frac{1}{m^*_{e^-}} + \frac{1}{m^*_{h^+}} \right] - \frac{1.8e^2}{\epsilon R} + \frac{e^2}{R} \sum_{n=1}^{\infty} \alpha_n \left( \frac{S}{R} \right)^{2n} \quad (9)$$

Figure 1 shows the energy of the lowest excited electronic state (i.e., the conduction band plus the transition recombination energy at the peak photoluminescence wavelength) versus the small iodide cluster diameter (R). The optical frequency dielectric for AgI (486 nm),  $\epsilon = 5.419$ ,

is inserted in the Coulomb attraction term and the third solvation energy loss term is not applicable. The effective masses  $m_{e^-}$ ,  $m_{h^+}$  of electrons and holes are approximated from literature values by comparing semiconductor properties. Silver bromide effective masses have been used as a reference. In general, it is shown that the smaller cluster size, the greater the band state; the wider the band, the smaller the effective mass.

Figures 2 and 3 show band edge positions of semiconductors<sup>8c,d</sup> with respect to AgBr, AgCl, and  $\beta\text{AgI}$ . The positions are given both as potentials<sup>8a,b</sup> versus NHE and as energies versus the electron in vacuum. The dashed lines are of data from different analytical procedures in comparison to the solid lines as noted previously.

Figures 4-12 are graphic interpretations of band positions of AgBr, AgBr,I, AgCl, and  $\beta\text{AgI}$  with respect to NHE potentials<sup>8a,b</sup> and as energies versus the electron in vacuum. The band gap positions are also related to redox couples in aqueous solutions.<sup>18</sup> The reduction by the photoexcited conduction band electron can take place when the redox couple lies below the bottom of the silver halide conduction band edges; and oxidation occurs by a valence band hole when the couple lies above the top of the valence band edge. Likewise, each of the semiconductors (Figures 2 and 3) is subject to the photo-oxidation and reduction processes similar to the silver halide materials in order to present new imaging systems.

The experimental data of  $I_m^{n-}$ , A-H solid lines describes the AgBr,I cryogenic photoluminescence involving  $I_m^{n-}$  in the region ~500 nm to 620 nm originating from the conduction band position of 3.30 eV.<sup>13</sup> The dashed lines represent conduction energy band reference levels for the recombination emission to the iodide cluster centers (also dashed lines A-H). Recently, Ehrlich has related an iodide shallow electron trapping center, 0.065 eV, beneath the conduction band of AgBr,I microcrystallites by activation energy determination from low-temperature photoluminescence measurements.<sup>16</sup> Also noted<sup>17</sup> within the AgCl,  $I_m^{n-}$  clusters were the recombination photoluminescence emissions of several complexes between 5.63 and 5.72 eV. Multitudes of redox couples are available within this range as seen in column I<sup>n-</sup> #31.

## Conclusions

1. The author has related silver halide band gap energies to the common reference vacuum level and also indicated the standard potential for redox couples referenced to the normal hydrogen electrode. This relationship suggests the thermodynamic limitations for photoreactions that can be carried out with charge carriers in the photographic silver halide microcrystals and other semiconductor materials of known band gap values.

2. If reduction of a chemical species, quantum cluster, nanocluster, or aggregate in or on the silver halide host is to be reduced, the conductive band position of the silver halide (which is photoexcited) must be positioned above the

relevant redox level to form a metastable state with the silver halide defect lattice.

3. Development of the silver-complex latent image may be internal to the grain or upon the surface at the interface of the aggregate or cluster.

4. The lowest unoccupied molecular orbital (LUMO) of the photon-absorbing adsorbed species cluster, or core semiconductor shelled or epitaxially placed upon silver halide, must be energetically positioned above the conduction band of the silver halide for photocatalysis of silver halide to occur.

5. Oxidation by a valence band silver halide hole occurs when the nonexcited couple (HOMO) highest occupied molecular orbital or semiconductor valence band lies above the photoexcited silver halide valence band.

6. Literature values (ESR) of shallow electron traps 0.446, 0.420, and 0.460 eV<sup>19</sup> of iridium III hexachloride under the conduction band (also 0.2 eV beneath (TSC) the conduction band<sup>20</sup>) would not distinguish the validity of the band gap measurements due to the activation energy reference to the conduction band. An activation energy also determined the positioning of the shallow trap at an emitting iodide center, 0.065 eV beneath the AgBr conduction band.

7.  $\text{Rh}(\text{CN})_6^{3-}/\text{Rh}(\text{CN})_6^{4-}$  ( $E^\circ = 0.9 \text{ V}$ ) show deeper electron trapping than experimental iridium III hexachloride, which correlated with photographic results.

## References

1. R. Meming, *Electroanalytical Chemistry*, Vol. 11, A. J. Bard, Ed., Marcel Dekker, New York, 1979.
2. J. O. M. Bockris and S. U. M. Khan, *J. Phys. Chem.*, 87, 2599 (1983).
3. F. Lohman, *Z. Naturforsch., Teil A*, 22, 813 (1956).
4. R. Gomer and G. Tryson, *J. Chem. Phys.*, 66, 4413 (1977).
5. S. Trasatti, *J. Electroanal. Chem.*, 139, 1 (1982).
6. S. Trasatti, *J. Electroanal. Chem.*, 209, 417 (1986).
7. R. S. Bauer and W. E. Spicer, *Phys. Rev. Lett.*, 25, 1283 (1970); R. S. Bauer and W. E. Spicer, *Phys. Rev. B*, 14, 4539 (1976); R. S. Bauer, Ph.D. Thesis, Stanford University, 1970.
8. (a) A. J. Bard, *Integrated Chemical Systems: A Chemical Approach to Nanotechnology*, John Wiley and Sons, New York, 1994. (b) A. J. Bard, R. Parsons, and J. Jordon, *Standard Potentials in Aqueous Solutions*, Marcel Dekker, Inc., New York, 1985; (c) N. Serpone and E. Pelizzette, *Photocatalysis, Fundamentals and Applications*, John Wiley and Sons, New York, 1989; (d) M. Grätzel, *Heterogeneous Photochemical Electron Transfer*, CRC Press, Boca Raton, FL, 1988.
9. J. Tejeda, N. I. Shevchik, W. Braun, A. Goldman, and M. Cardona, *Phys. Rev. B*, 12, 1557 (1975).
10. L. E. Brus, *J. Phys. Chem.*, 80, 4403 (1984); *ibid* 79, 5566 (1983).
11. L. E. Brus, *J. Phys. Chem.*, 90, 2555 (1986).
12. L. E. Brus, *J. Quantum Electron.*, 22, 1909 (1986).
13. S. H. Ehrlich, *J. Imaging Sci. Technol.*, 37, 73 (1993).
14. S. H. Ehrlich, *J. Imaging Sci. Technol.*, 38, 201 (1994).
15. S. H. Ehrlich, *J. Imaging Sci. Technol.*, 39, 97 (1995).
16. S. H. Ehrlich, *J. Imaging Sci. Technol.*, 41, 13 (1997).
17. S. H. Ehrlich and J. Edwards, *J. Imaging Sci. Technol.*, 43, 15 (1999).
18. D. R. Lide, Ed., *CRC Handbook of Chemistry and Physics*, 74<sup>th</sup> Edition, CRC Press, Boca Raton, FL, 1993-1994, pp. 8-21 to 8-31.
19. R. S. Eachus and M. T. Olm, *Cryst. Lattice Defects Amorphous Mater.*, 18, 297 (1989).
20. L. M. Kellog, unpublished data, Eastman Kodak Company.

## Biography

Dr. Sanford H. Ehrlich received his B.Sc. in biology and chemistry from New York University and his M.Sc. in theoretical electrochemistry in 1957 from the same university after his service in Korea. His research for his doctoral thesis was in the area of molecular surface spectroscopy investigating adsorption phenomena of polyelectrolytes. He received his Ph.D. in 1962 from Adelphi and New York University. From 1963-1965 he carried out conductivity studies in materials at cryogenic temperatures at Air Products Co., PA. In 1965-1967, as a senior researcher at the American Optical Co., MA, he investigated and invented variable transmission glasses via studying defect properties of glass. In 1967, he moved to Eastman Kodak Company's Research Laboratories. From 1967-1972, he investigated the sensitization and electron transfer properties in electrophotographic systems. Non-light-sensitive direct X-ray imaging systems were of interest. From 1972-1979, his efforts were directed to electron transfer processes involving spectral, chemical, and dopant sensitization of silver halides, using pulsed relaxation transient spectroscopy. During this period he invented surface coatings for finish glass lens molding and new aspherical pre-form glass processes for molding lens. Since 1979, he has developed novel techniques in laser microwave photoconductivity and fluorescence to investigate electron trapping in the solid state. He has applied these technologies to mechanistic studies relating to imaging processes in silver halide and other systems. He has been involved in chemiluminescent systems for diagnostic biochemistry. The most recent studies involve spectroscopic low-temperature photoluminescent investigations with quantum-sized clusters of iodide, silver, and silver sulfides in silver halide systems; also, kinetic processes of formation and electron-trapping efficiencies of quantum-sized clusters silver halide clusters in gelatin matrices using stopped-flow and sequential techniques.

Dr. Ehrlich has also taught advanced courses in physics/biophysics, physical, photo, inorganic, and biochemistry at the University of Rochester and Rochester Institute of Technology over a period of 25 years. In May 1993, he was selected as a Fellow of the Society for Imaging Science and Technology. The award was in recognition of fundamental work towards understanding of the mechanisms of dopants and dye sensitization of silver halides. He also received the Journal Award (Science) for outstanding contributions in the area of basic sciences for the scientific

paper entitled "Spectroscopic Studies of AgBr with Quantum-sized Clusters of Iodide, Silver, and Silver Sulfides" in 1994. In 1998, Dr. Ehrlich was awarded the prestigious Lieven Gevaert Medal for his many contributions in spectroscopic analysis of silver halide and related imaging processes. This award is sponsored by Bayer Corporation/Agfa Division, which recognizes outstanding contributions in the field of silver halide photography.

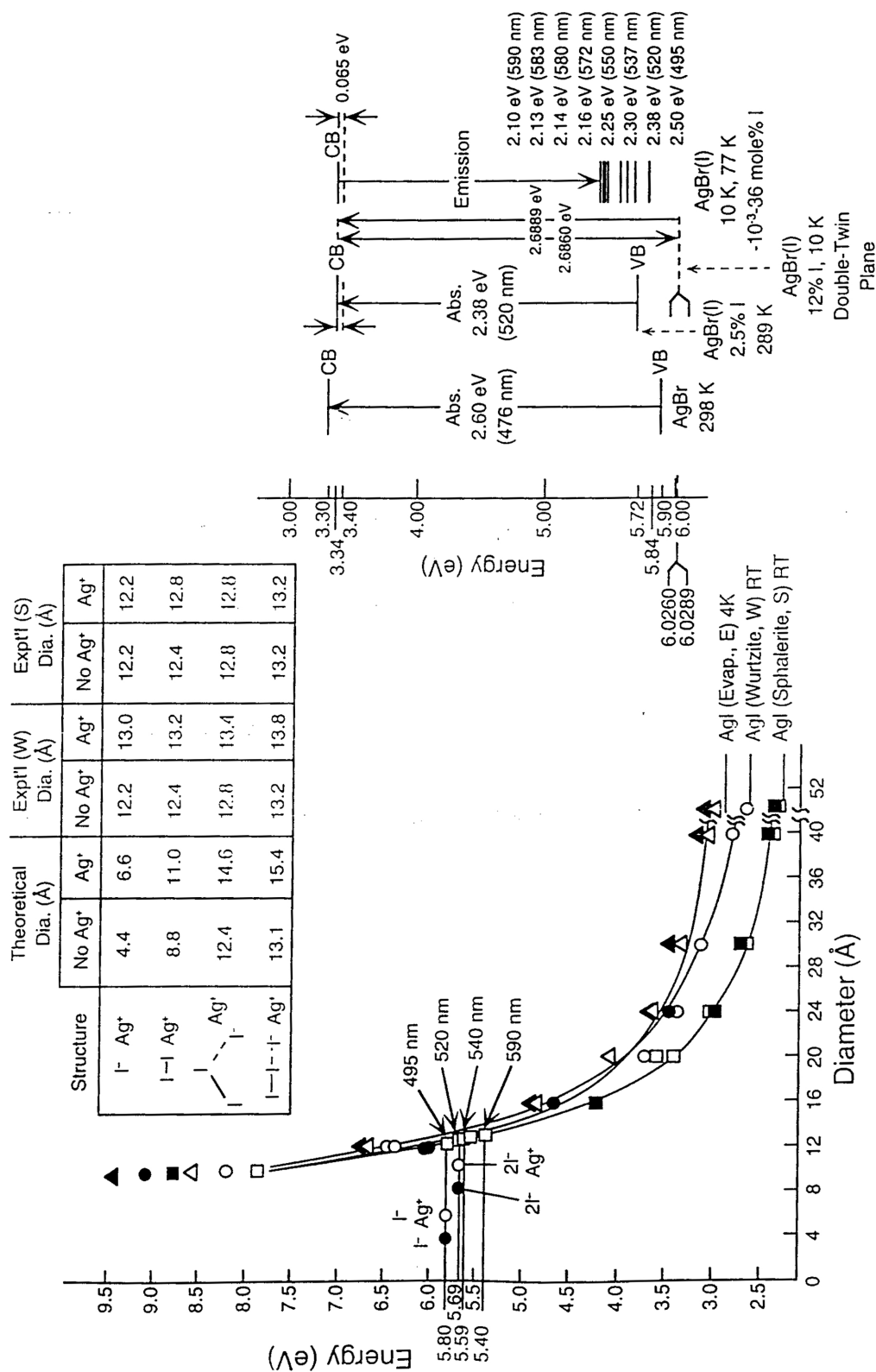


Figure 1. The energy of the lowest excited electronic state; i.e., the conduction band plus the transition recombination energy at the peak photoluminescence wavelength, versus the small iodide cluster diameter,  $R$ .

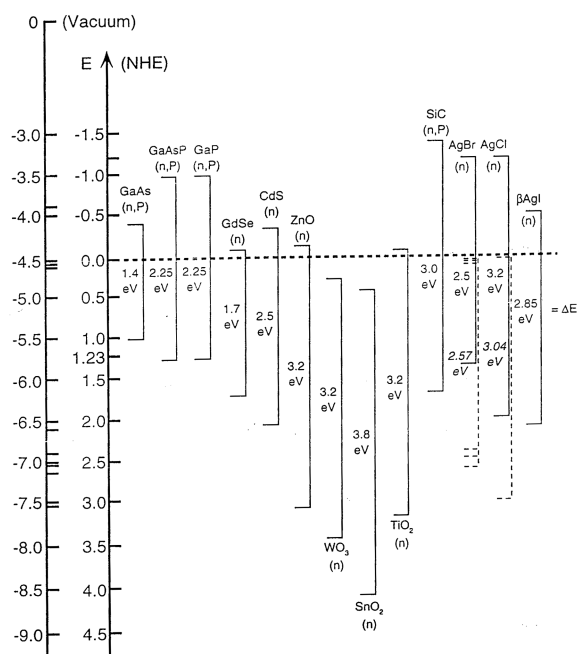


Figure 2

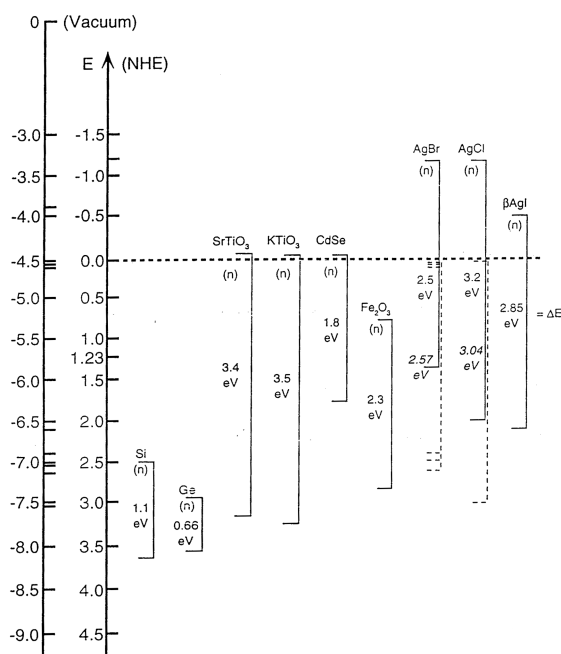


Figure 3

Figures 2 and 3. The band positions of semi-conductors with respect to AgBr, AgCl, and  $\beta$ AgI. The positions are given both as potentials versus NHE, and as energies versus the electron in vacuum. The dashed lines are of data from different analytical procedures or state of the materials than the solid lines as noted previously.

Figures 4-12. Graphic interpretations of band positions AgBr, AgCl, and  $\beta$ AgI with respect to NHE potentials and as energies versus the electron in vacuum. The band gap positions are also related to different redox couples in aqueous solutions.

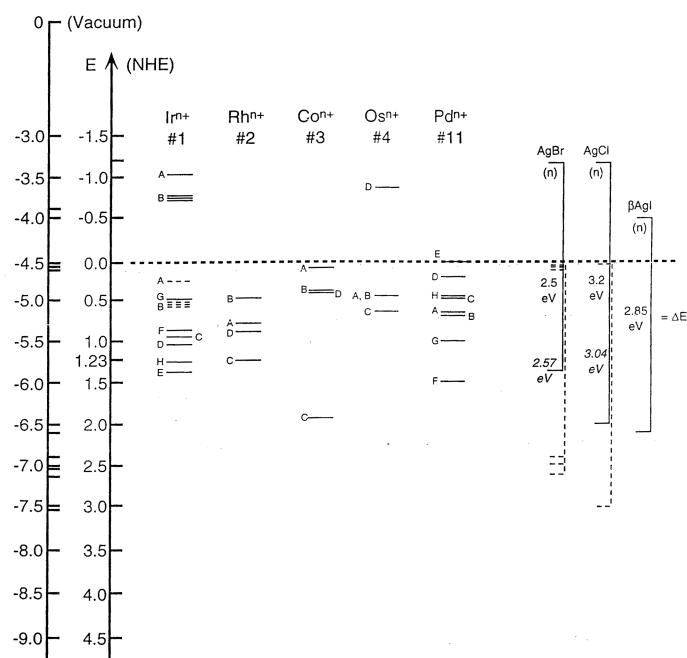


Figure 4

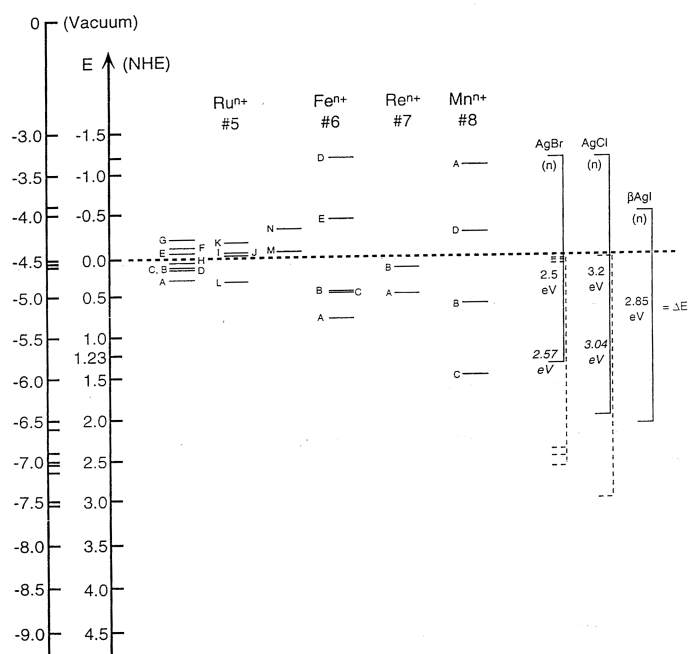


Figure 5

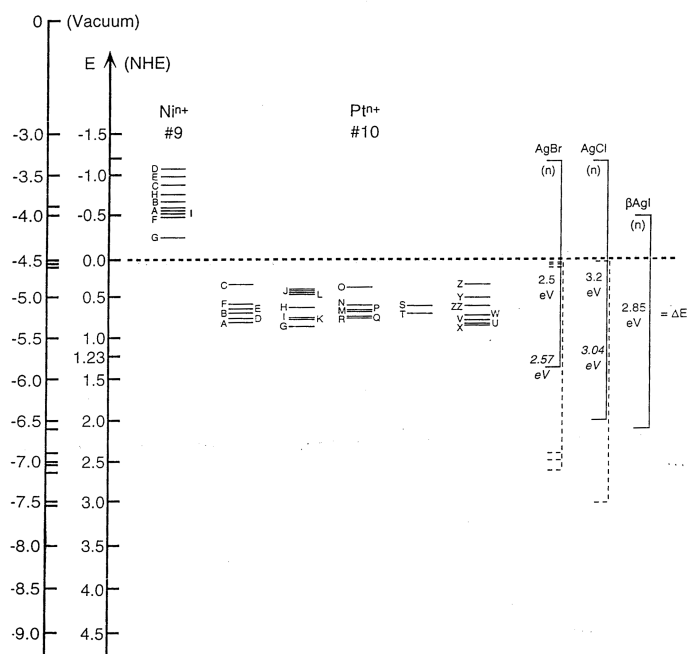


Figure 6

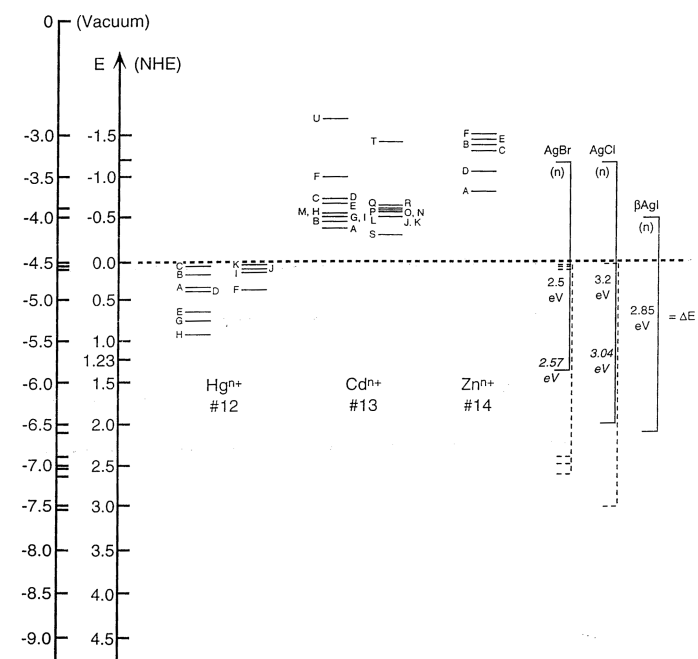


Figure 7



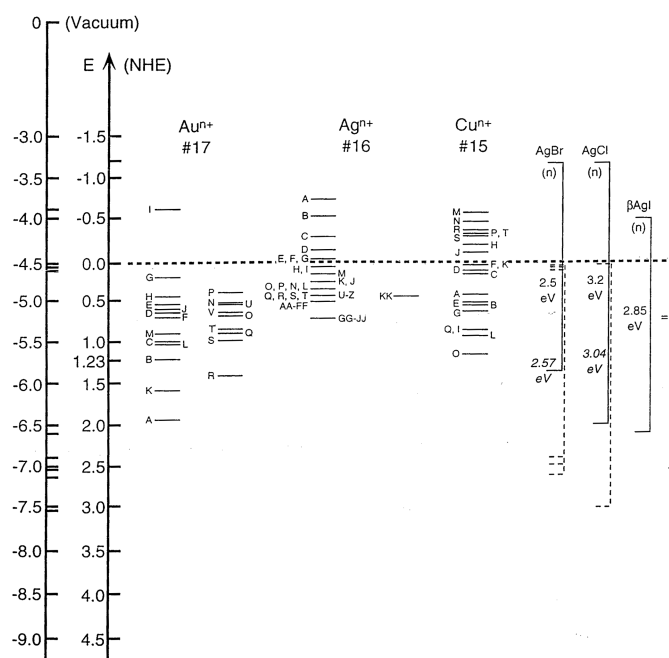


Figure 8

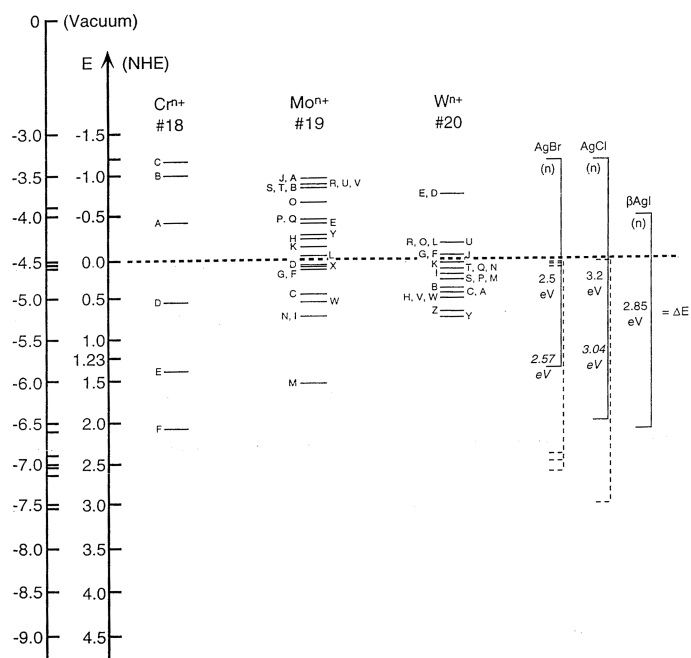
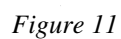
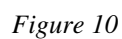


Figure 9



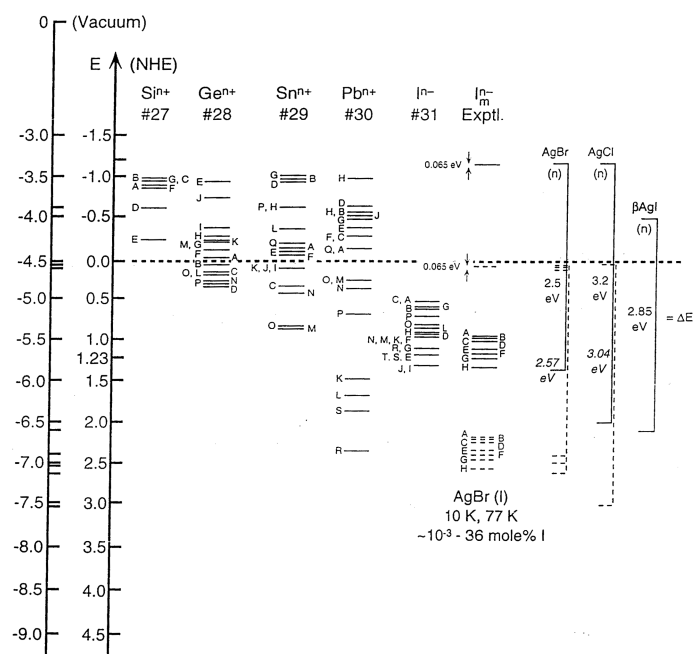


Figure 12